

Short Communication

Electrochemical Analysis of Corrosion Behavior $\text{Al}_2\text{O}_3\text{-ZrO}_2$ Ceramic Layer Coated Carbon Steel Pipes for Potential Oil Exploitation Application

Yisheng Hu^{1*}, Ziyi Wang², Haohan Liu³

¹ State Key Laboratory of Oil and Gas Reservoir Geology and Exploitation, Southwest Petroleum University, Chengdu 610500, Sichuan, China

² Exploration & Production Institute of Southwest Petroleum Branch Company, SINOPEC, Chengdu, Sichuan, 610041, China

³ Sichuan College of Architectural Technology, Deyang, 618000, China

*E-mail: huyisheng008@yahoo.com

Received: 25 July 2016 / Accepted: 19 September 2016 / Published: 10 October 2016

$\text{Al}_2\text{O}_3\text{-ZrO}_2$, which is ceramic composite exhibiting high corrosion stability, is coated on the surface of Q235 carbon steel pipes through plasma spray and high velocity oxy-fuel spray (HOVF) methods. The thick and homogenous deposited layers can be generated by these approaches, whereas the influence of these methods on the properties of the materials are negligible. The resistant performance of coated samples to corrosion is studied in the mixture of the simulated seawater and crude oil for 60 days. Then, according to the analysis by electrochemical impedance spectroscopy, the $\text{Al}_2\text{O}_3\text{-ZrO}_2$ coated samples prepared by plasma spray method display high corrosion resistance than those produced by HVOF. However, both these two approaches exhibit a protection on carbon steel in corrosive environment. Based on XRD and SEM analysis, it is demonstrated that the substrate could not be reached by the solution.

Keywords: Plasma coating technique; HOVF; Electrodeposition; EIS; $\text{Al}_2\text{O}_3\text{-ZrO}_2$

1. INTRODUCTION

The environments of offshore oil production are characteristic of aggressive conditions such as corrosion and erosion. Corrosion-erosion, primarily at gravel packs, nozzles and Christmas trees, can cause up to 15% loss in oil and gas production, even before hydrocarbons arrive at the first separator [1]. However, the deterioration rate of metal is accelerated by this phenomenon, owing to the combined effect of electrochemical etching and mechanical erosion. This combined influence, known as synergy, can result in higher metal loss rate and greater damage than erosion or corrosion alone. Therefore, the lifetime of components can be shortened remarkably by this effect [2, 3]. Moreover,

owing to their high mechanical properties and machinability at low price, the carbon steels have extensively been applied in oil well. However, in a large extent, the poor corrosion resistance of carbon steel restricts their further applications, particularly in aggressive conditions. Thus, a variety of approaches, such as corrosion inhibitor method, cathodic protection and covering the coatings or films on the steels, are used to protect the carbon steels against corrosion [4]. Depositing the shielded coating onto the surface of carbon steel becomes one of the most widespread approach to decrease the corrosion rate [5, 6]. For preparing the coatings, numerous methods, such as chemical plasma spray, plasma electrolytic oxidation (PEO), sol-gel, vapour deposition (CVD), physical vapour deposition (PVD) and high velocity oxy-fuel (HVOF) spraying, could be employed [7-10].

A wide variety of materials, including metals, polymers and ceramics, can be sprayed onto the metal and ceramic substrates by thermal spray coating among them. This coating is built with the intent to enhance the engineering performance such as resistance to corrosion, wear or high temperature and increasing the component life [11]. The ceramic coatings are effective in various environments, where the resistance to corrosion and wear are necessary, particularly in an elevated temperature condition, whereas the other coatings could reach [12-14]. For instance, alumina and zirconia coatings are applied increasingly and widely in the area of industry to supply resistance to wear and erosion, thermal insulation and corrosion protection [15, 16]. The defects existing in the ceramic coatings sprayed by plasma are harmful to the corrosion resistance of the coating systems, although the coating materials possess the feature of high corrosion resistance in nature [17-19]. Defects in the coating are definitely toxic, as they provide direct pathways for corrosive electrolytes to go through the coating and reach the surface of substrate [20, 21].

Among all the thermal spray methods, Plasma and HVOF spray are two of the most widespread ones. In prior to being projected onto a substrate at high velocity, the heated particles are sprayed by a flame (plasma or oxygen-fuel). Then, the particles flatten to form splats by impact, which form the coating ultimately. Such processes serve to achieve substrate surface modifications. However, the difficulties to carry out high-magnification analysis of the boundary between the splat and the substrate hinder from understanding the mechanism of the splat formation and the interactions between the splat and the substrate [22-24].

Electrochemical impedance spectroscopy (EIS) is an effective analysis method, which has already been demonstrated to be useful to analyse the localized corrosion of the coated steel systems [25, 26]. Herein, we deposited successfully the $\text{Al}_2\text{O}_3\text{-ZrO}_2$ ceramic composite on the surface of oil piping through plasma and HVOF methods. EIS was used to evaluate the corrosion resistance of Q235 carbon steel. Meanwhile, scanning electron microscopy (SEM) and X-ray diffraction (XRD) were used to characterize their microstructures.

2. EXPERIMENTS

2.1. Materials

The substrate made of Q235 carbon steel was machined into the small samples with the size of 10 mm × 10 mm × 15 mm. The powders of Al_2O_3 and ZrO_2 with the size of 50-80 nm were

commercially obtained from Tianjing Ceramic Company. To improve the adhesive bond between the substrate and the coating, the pure 36grit Al_2O_3 was used to degrease and grit blast the carbon steel samples under the blasting pressure of above 50 MPa. Then the samples were cleansed by ultrasonic with alcohol and acetone.

2.2. Plasma and HVOF coating

The Al_2O_3 - ZrO_2 powders were sprayed onto the surface of carbon steel substrate in the ratio of 1:1 by plasma thermal spray and HVOF methods. Noted that the substrate was preheated at 75-85 °C to eliminate oxidation before conducting deposition. The primal parameters of these two coating techniques are shown in Table 1.

Table 1. The main plasma spraying and HVOF parameters.

Method	Voltage (V)	Substrate velocity (m/s)	Current (A)	Gun traverse speed (mm/s)	Spraying distance (mm)	Gas flow rate (L/min)
Plasma thermal spray	120	—	480	—	120	Ar:75 H ₂ :130
HVOF	—	1	—	5	200	O ₂ :150 Propylene:100

2.3. Characterization

The scanning electron microscopy (SEM, ZEISS X-MAX) was used to study the morphology and microstructure of the surface coatings. The XRD spectra of the coated pipe was obtained in the range of 20° to 80° in 2θ by XRD (PW3040/60 X'pert PRO).

2.4. Electrochemical corrosion test

The electrochemical corrosion test was carried out in the following steps. First, the surface of bare samples for test without coatings had the copper conducting wires welded on. Subsequently, epoxy resin was inset into the samples with only 1 cm² exposed area for coatings left. Then the electrochemical corrosion tests were carried out in the three-electrode cell, where the graphite, the saturated calomel electrode (SCE) and the coated samples were used as the counter electrode, the reference electrode and the working electrode, respectively. Moreover, the electrolyte was consisted of the crude oil and the simulated seawater which contains 96.5 wt.% H₂O, 2.73 wt.% NaCl, 0.24 wt.% MgCl₂, 0.34 wt.% MgSO₄, 0.11 wt.% CaCl₂ and 0.08 wt.% KCl. The immersion times were set as 3, 10, 20, 40, 60 days. The EIS spectra was collected at the open circuit potential of coating samples, when the signal amplitude is 10 mV rms and the frequency is in the range of 0.01 to 100,000 Hz. The EIS fitting software (ZSimp Win) was used to fit and interpret the EIS data. SEM was used to analyse the corroded samples after long-time dip. Noted that all sets of measurements were repeated for three times to confirm the repeatability.

3. RESULTS AND DISCUSSION

The typical microstructures of $\text{Al}_2\text{O}_3\text{-ZrO}_2$ coatings prepared by plasma and HVOF spray are shown in Figure 1. A dense microstructure exhibiting high cohesion was obtained when depositing the powder of this composite on the surface of carbon steel. However, some pores were observed through micrograph in the shape of black spots. It is reported that such pores were induced by the semi- and un-melted particles in $\text{Al}_2\text{O}_3\text{-ZrO}_2$ coatings, which could be recognized by the characteristic of spherical shape. Owing to the high-impact velocity of particles in the coating, this is considered low porosity, which could induce single splat with high density and cohesive strength [22]. The micrographs of the coating are shown in Figure 1, in which uniform, homogeneous and free-form surface cracks are observed. To improve the corrosion stability of $\text{Al}_2\text{O}_3\text{-ZrO}_2$ coating, preparing a whole and relatively homogenous coating is crucial. In addition, no obvious difference is observed in the coatings prepared by plasma and HVOF approaches.

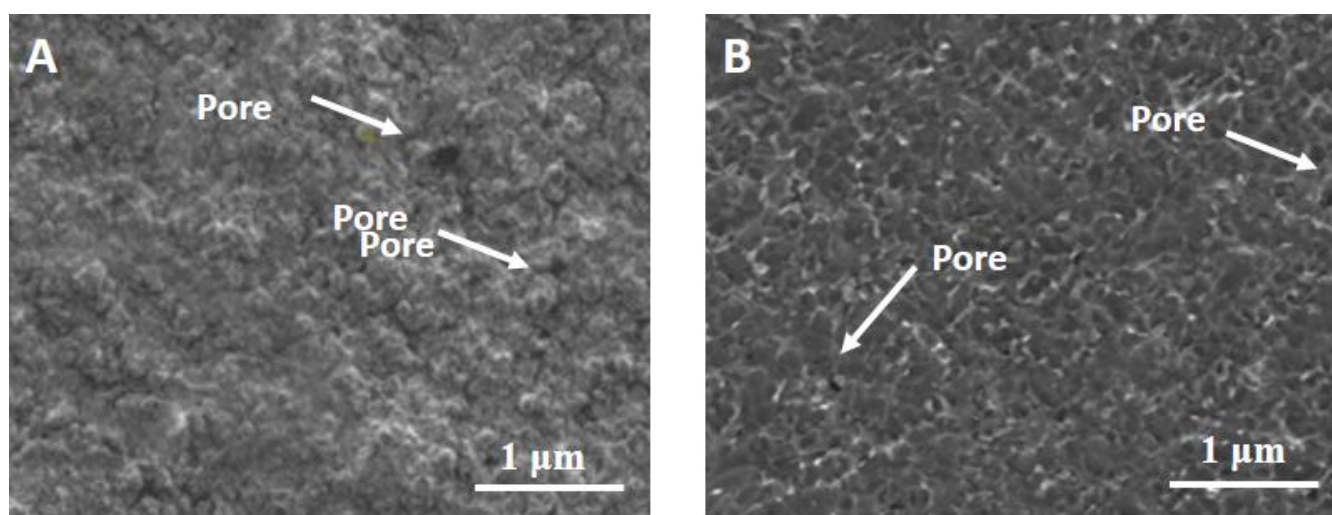


Figure 1. SEM of (A) plasma and (C) HVOF-sprayed $\text{Al}_2\text{O}_3\text{-ZrO}_2$ coated carbon steel.

XRD spectra of the as-formed $\text{Al}_2\text{O}_3\text{-ZrO}_2$ powders and coatings by these two techniques are shown in Figure 2. The as-formed powders are consisted of stable $\alpha\text{-Al}_2\text{O}_3$ and monoclinic- ZrO_2 phase, which are also observed in the initial powders. A similar pattern was observed in the XRD spectra of the as-formed coatings. However, phase transformations took place in the coatings. The presence of $\alpha\text{-Al}_2\text{O}_3$, $\gamma\text{-Al}_2\text{O}_3$, monoclinic and tetragonal- ZrO_2 in both the two $\text{Al}_2\text{O}_3\text{-ZrO}_2$ coatings. Owing to the less critical free energy needed for nucleation from liquid compared with $\alpha\text{-Al}_2\text{O}_3$, it indicated that the $\gamma\text{-Al}_2\text{O}_3$ nucleated homogeneously, when thoroughly molten droplets were quenched rapidly. The main phase observed in all the coatings was metastable $\gamma\text{-Al}_2\text{O}_3$, which was caused by the rapidly cooling after spraying procedure. It was reported that $\gamma\text{-Al}_2\text{O}_3$ possesses nanocrystalline, whereas $\alpha\text{-Al}_2\text{O}_3$ contains microcrystalline dimension [22]. Consequently, during the process of spraying, the $\alpha\text{-Al}_2\text{O}_3$ could remain and be embed in $\gamma\text{-Al}_2\text{O}_3$ matrix, which is partially melted.

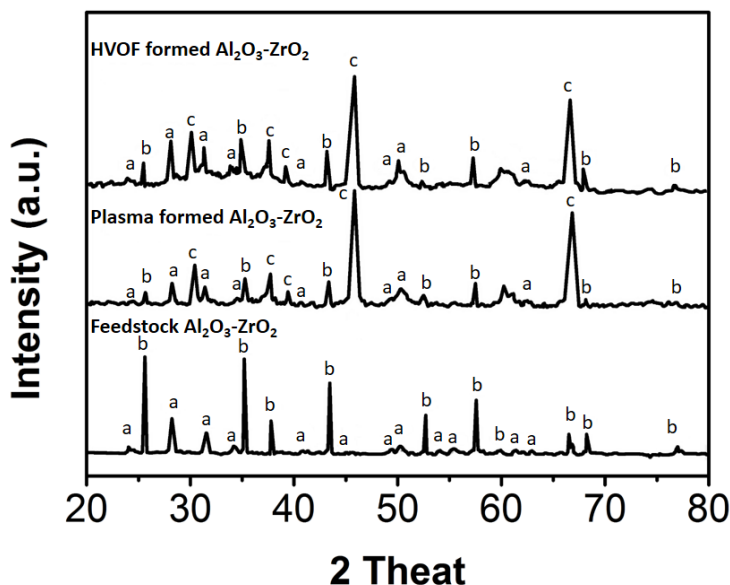


Figure 2. XRD patterns of feedstock $\text{Al}_2\text{O}_3\text{-ZrO}_2$ powders and $\text{Al}_2\text{O}_3\text{-ZrO}_2$ composite coatings formed by plasma and HVOF spray. (a: $\alpha\text{-Al}_2\text{O}_3$; b: Monoclinic ZrO_2 ; c: $\gamma\text{-Al}_2\text{O}_3$)

Electrochemical impedance spectroscopy was used to study the corrosion resistance of the $\text{Al}_2\text{O}_3\text{-ZrO}_2$ coatings. Figure 3 shows the obtained EIS data of $\text{Al}_2\text{O}_3\text{-ZrO}_2$ coating samples illustrated in Nyquist spectra, where the samples produced through plasma and HVOF spray methods were immersed in the mixture of simulated seawater and crude oil. It was obvious that the EIS spectra of these two coatings showed a similar pattern. This indicated that these two coatings possessed similar electrochemical corrosion mechanism. Other report also indicates the plasma and HVOF spray methods formed ceramic coatings will show similar corrosion mechanism [27].

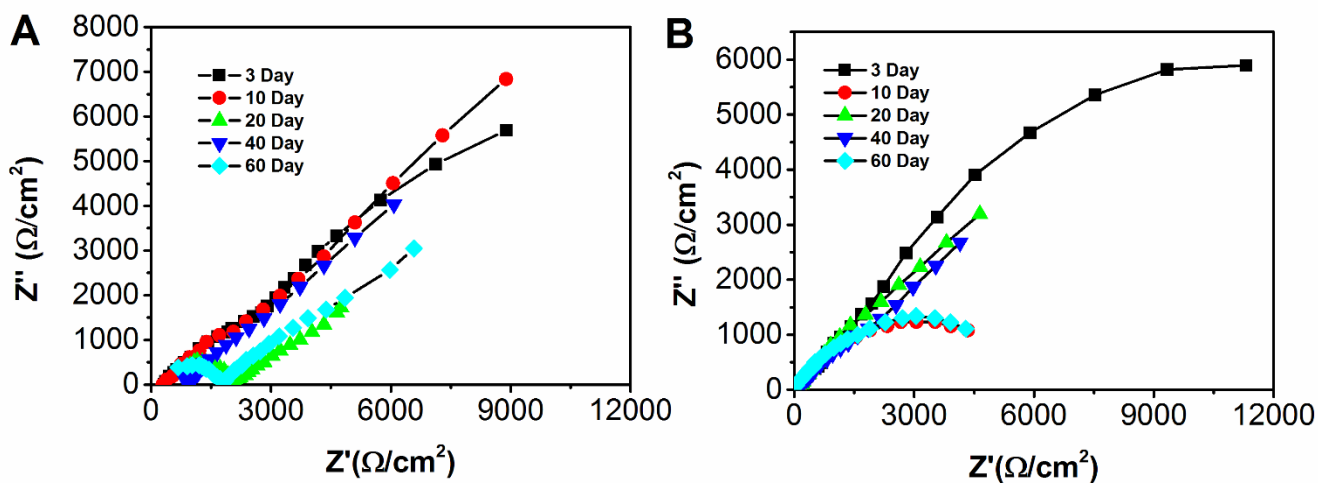


Figure 3. Nyquist spectra of the (A) plasma and (B) HVOF-sprayed $\text{Al}_2\text{O}_3\text{-ZrO}_2$ after different immersion time in simulated seawater mixed with crude oil.

However, different corrosion mechanisms took place in both the coatings at the earlier stage and later stage of dipping process. Two obvious capacitive loops were observed in Nyquist plots after 3-day immersion. It suggested that two time constants present in the system. The corrosion process could be represented by the low-frequency loop, whereas the high-frequency loop could be attributed physically to the defects in the coatings [26]. However, for later stage of immersion, the feature of the Nyquist plots changed, where a straight line was also observed at low frequency because of the generated Warburg impedance. A similar phenomenon has been reported by Liu et al [28]. The straight line appeared due to the Warburg impedance created.

Figure 4 shows the equivalent circuits, which are used to fit and interpret the EIS data of the two coatings, because of their microstructures and typical EIS. The electrochemical corrosion mechanism of the two coatings changed when increasing the time of immersion. The $\text{Al}_2\text{O}_3\text{-ZrO}_2$ coating generated by plasma spray could be fitted by the equivalent circuit in Figure 4A, when the equivalent circuit in Figure 4B could interpret the $\text{Al}_2\text{O}_3\text{-ZrO}_2$ coating prepared by HVOF [29, 30]. The solution resistance between the reference electrode and the coated surface is illustrated in R_s , which is connected with one-time constants in parallel arrangement of R and Q [31]. Table 2 shows the R_{ct} of carbon steel coated with $\text{Al}_2\text{O}_3\text{-ZrO}_2$ immersed for 3 to 60 days, which were prepared through plasma and HVOF spray. It is obviously shown in Table 2 that after being immersed for 3 days the corrosion current I_{corr} of carbon steel was $78.55 \mu\text{A}$, while in the end of the immersion the current changed to $420.8 \mu\text{A}$. It indicated that the earlier stage and the later stage behaved differently. Moreover, it is obvious in Table 2 that R_{ct} value of the samples prepared by plasma spray is larger than that of HVOF coated samples in almost all the measurements. These results demonstrated that the coating prepared by plasma spray exhibited a higher corrosion protection of the surface of carbon steel compared to that generated through HVOF. Moreover, the corrosion current density of the samples coated by plasma increased a bit from $0.7414 \mu\text{A}$ on the third day to $0.8301 \mu\text{A}$ on tenth day. However, the current density of the samples generated by HVOF only fluctuated in this period, where the current first increased from $0.7414 \mu\text{A}$ on the third day to $0.7584 \mu\text{A}$ on the 20th day, then it plunged to $0.7764 \mu\text{A}$ on the 40th day and fluctuated to $0.7906 \mu\text{A}$ on the 60th day.

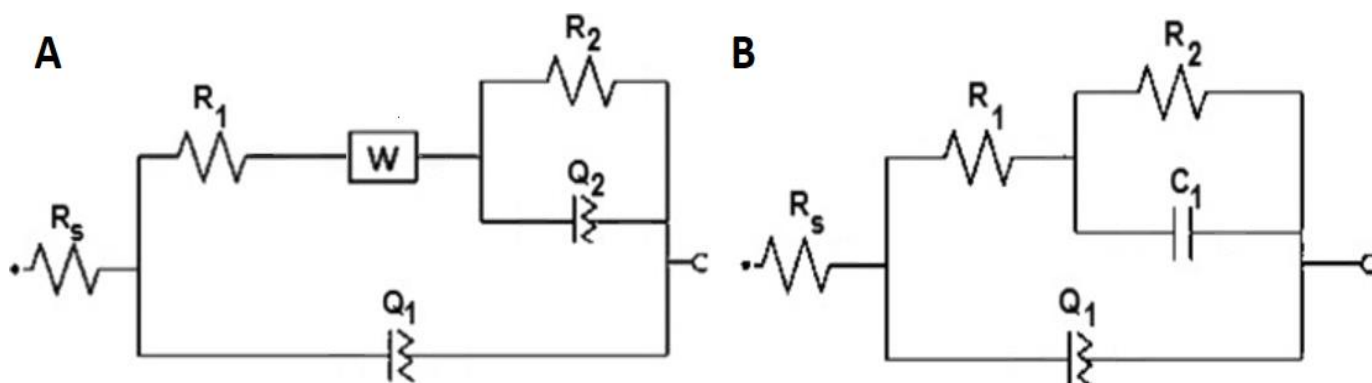
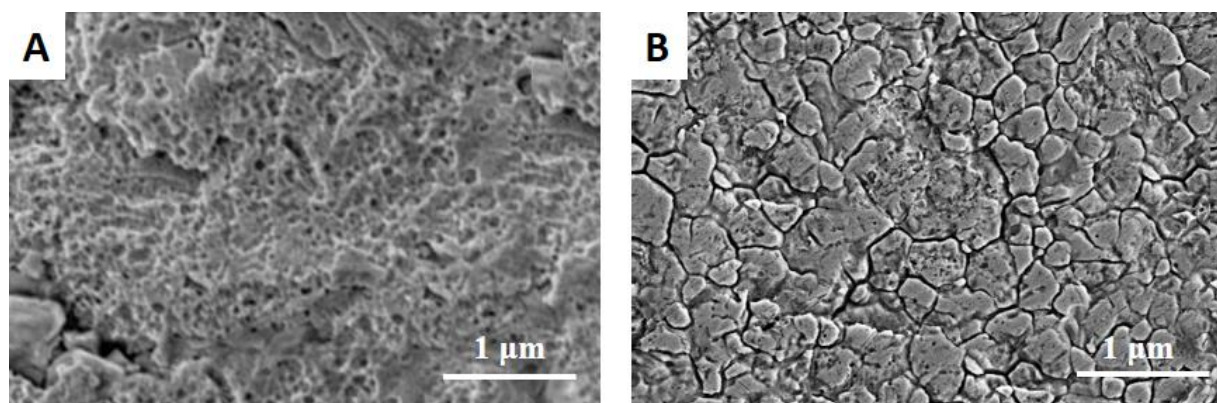


Figure 4. Equivalent circuits for EIS of the (A) plasma sprayed $\text{Al}_2\text{O}_3\text{-ZrO}_2$ and (B) HVOF sprayed $\text{Al}_2\text{O}_3\text{-ZrO}_2$.

Table 2. I_{corr} and R_{CT} of carbon steel, $\text{Al}_2\text{O}_3\text{-ZrO}_2$ samples with plasma and HVOF coating methods in simulated seawater mixed crude oil for 60 days.

Day	Carbon steel		Plasma coated Sample		HVOF coated Sample	
	$I_{\text{corr}}/\mu\text{A}$	$R_{\text{CT}}/\text{k}\Omega$	$I_{\text{corr}}/\mu\text{A}$	$R_{\text{CT}}/\text{k}\Omega$	$I_{\text{corr}}/\mu\text{A}$	$R_{\text{CT}}/\text{k}\Omega$
3	78.55	2.588	0.7422	21.524	0.7414	22.124
10	135.4	2.421	0.7584	21.332	0.7465	21.754
20	248.6	2.245	0.7693	21.278	0.7584	21.661
40	398.6	2.101	0.7989	21.178	0.7764	21.443
60	420.8	2.004	0.8214	21.107	0.7906	21.228

The SEM images of the top surface of $\text{Al}_2\text{O}_3\text{-ZrO}_2$ coatings prepared through plasma and HVOF approaches were illustrated in Figure 5, where the coatings were dipped in the mixture of simulated seawater and crude oil for 60 days. The corrosion damage was observed obviously in both the coatings from the SEM images. Moreover, due to the damaged initial micro pores, the cracks and pores in the coatings became considerably larger. It is obvious that serious local corrosion present in both the samples. However, compared to the $\text{Al}_2\text{O}_3\text{-ZrO}_2$ coating prepared by HVOF, a relatively slighter corrosion took place in the $\text{Al}_2\text{O}_3\text{-ZrO}_2$ coating produced by plasma spray. A similar result has been reported by Zavareh et al [27]. The carbon steel shows a significant difference between the corroded and un-corroded surfaces. The violent corrosion, particularly pitting corrosion, occurred on carbon steel in crude oil after 30days and destroyed the substrate surface.

**Figure 5.** SEM image of $\text{Al}_2\text{O}_3\text{-ZrO}_2$ coatings prepared using (A) plasma and (B) HVOF spray methods after immersion in simulated seawater mixed with crude oil for 60 days.

4. CONCLUSIONS

In conclusion, we prepared $\text{Al}_2\text{O}_3\text{-ZrO}_2$ coated carbon steel through plasma and HVOF spray approaches, which was analyzed by electrochemical investigation. The results indicated that $\text{Al}_2\text{O}_3\text{-ZrO}_2$ had a remarkable effect on the corrosion performance of carbon steel. Furthermore, based on the corrosion test, where the samples were placed in the mixture of the simulated seawater and crude oil for 60 days, the $\text{Al}_2\text{O}_3\text{-ZrO}_2$ coated sample prepared by plasma exhibited higher corrosion stability than that produced through HVOF.

References

1. N. Espallargas, J. Berget, J. Guilemany, A.V. Benedetti and P. Suegama, *Surface and Coatings Technology*, 202 (2008) 1405
2. J. Guilemany, N. Espallargas, P. Suegama and A.V. Benedetti, *Corrosion Science*, 48 (2006) 2998
3. P. Kulu, I. Hussainova and R. Veinthal, *Wear*, 258 (2005) 488
4. J. Kawakita, T. Fukushima, S. Kuroda and T. Kodama, *Corrosion Science*, 44 (2002) 2561
5. D. Toma, W. Brandl and G. Marginean, *Surface and Coatings Technology*, 138 (2001) 149
6. G. Ruhi, O. Modi, A. Sinha and I. Singh, *Corrosion science*, 50 (2008) 639
7. F. Guidi, G. Moretti, G. Carta, M. Natali, G. Rossetto, Z. Pierino, G. Salmaso and V. Rigato, *Electrochimica acta*, 50 (2005) 4609
8. A.S. Hamdy, D. Butt and A. Ismail, *Electrochimica acta*, 52 (2007) 3310
9. T. Sundararajan, S. Kuroda and F. Abe, *Corrosion science*, 47 (2005) 1129
10. Z. Liu, Y. Dong, Z. Chu, Y. Yang, Y. Li and D. Yan, *Materials & Design*, 52 (2013) 630
11. M. Magnani, P. Suegama, N. Espallargas, C.S. Fugivara, S. Dosta, J. Guilemany and A.V. Benedetti, *Journal of Thermal Spray Technology*, 18 (2009) 353
12. Y. Wang, S. Jiang, M. Wang, S. Wang, T.D. Xiao and P.R. Strutt, *Wear*, 237 (2000) 176
13. D. Yan, J. He, J. Wu, W. Qiu and J. Ma, *SURFACE & COATINGS TECHNOLOGY*, 89 (1997) 191
14. V.P. Singh, A. Sil and R. Jayaganthan, *materials & Design*, 32 (2011) 584
15. O. Sarikaya, *Materials & design*, 26 (2005) 53
16. A. Afrasiabi, M. Saremi and A. Kobayashi, *Materials Science and Engineering: A*, 478 (2008) 264
17. P. Ctibor, K. Neufuss, F. Zahalka and B. Kolman, *Wear*, 262 (2007) 1274
18. H.-J. Kim, C.-H. Lee and Y.-G. Kweon, *Surface and Coatings Technology*, 139 (2001) 75
19. P. Suegama, C.S. Fugivara, A.V. Benedetti, J. Fernández, J. Delgado and J. Guilemany, *Corrosion Science*, 47 (2005) 605
20. X. Zhao, D. Yan, S. Li and C. Lu, *Appl. Surf. Sci.*, 257 (2011) 10078
21. S. Liscano, L. Gil and M.H. Staia, *Surface and Coatings Technology*, 188 (2004) 135
22. J. Murthy and B. Venkataraman, *Surface and Coatings Technology*, 200 (2006) 2642
23. D. Poirier, J.-G. Legoux and R.S. Lima, *Journal of thermal spray technology*, 22 (2013) 280
24. M. Akhtari Zavareh, A.A.D. Mohammed Sarhan, P. Akhtari Zavareh and W.J. Basirun, *Ceram. Int.*, 42 (2016) 3397
25. C. Liu, Q. Bi, A. Leyland and A. Matthews, *Corrosion Science*, 45 (2003) 1257
26. Z. Yao, Z. Jiang, S. Xin, X. Sun and X. Wu, *Electrochimica Acta*, 50 (2005) 3273
27. M.A. Zavareh, A.A.D.M. Sarhan, P.A. Zavareh and J.B. Wan, *Ceram. Int.*, 42 (2015) 3397
28. Z. Liu, Y. Dong, Z. Chu, Y. Yang, Y. Li and D. Yan, *Materials & Design*, 52 (2013) 630
29. M. Li, S. Luo, C. Zeng, J. Shen, H. Lin and C.n. Cao, *Corrosion science*, 46 (2004) 1369
30. V.W. Grips, H.C. Barshilia, V.E. Selvi and K. Rajam, *Thin solid films*, 514 (2006) 204
31. M.A. Zavareh, A.A.D.M. Sarhan, P.A. Zavareh and W.J. Basirun, *Ceram. Int.*, 42 (2016) 3397